Tunneling spectroscopy of few-monolayer NbSe2 in high magnetic fields
Triplet superconductivity and Ising protection

Kuzmanović, M.; Dvir, T.; Leboeuf, D.; Ilić, S.; Haim, M.; Möckli, D.; Kramer, S.; Khodas, M.; Meyer, J. S.; More Authors

DOI
10.1103/PhysRevB.106.184514

Publication date
2022

Document Version
Final published version

Published in
Physical Review B

Editors' Suggestion

Tunneling spectroscopy of few-monolayer $NbSe_2$ in high magnetic fields: Triplet superconductivity and Ising protection

M. Kuzmanović,[1,2,*] T. Dvir,[3,4,*] D. LeBoeuf,[5] S. Ilić,[6,7] M. Haim,[3] D. Möckli,[3,8] S. Kramer,[5] M. Khodas,[3] M. Houzet,[6] J. S. Meyer,[6] M. Aprili,[1] H. Steinberg,[3] and C. H. L. Quay[1,†]

[1]*Laboratoire de Physique des Solides (CNRS UMR 8502), Bâtiment 510, Université Paris-Saclay, 91405 Orsay, France*
[2]*QTF Centre of Excellence, Department of Applied Physics, Aalto University School of Science, P.O. Box 15100, 00076 Aalto, Finland*
[3]*Racah Institute of Physics, Hebrew University of Jerusalem, Givat Ram, Jerusalem 91904, Israel*
[4]*QuTech and Kavli Institute of Nanoscience, Delft University of Technology, 2600 GA Delft, The Netherlands*
[5]*Laboratoire National des Champs Magnétiques Intenses (LNCMI-EMFL), CNRS, Université Grenoble Alpes, UPS, INSA, 38042 Grenoble, France*
[6]*Université Grenoble Alpes, CEA, Grenoble INP, IRIG, PHELIQS, 38000 Grenoble, France*
[7]*Centro de Física de Materiales (CFM-MPC), Centro Mixto CSIC-UPV/EHU, 20018 Donostia–San Sebastián, Spain*
[8]*Instituto de Física, Universidade Federal do Rio Grande do Sul, 91501-970 Porto Alegre, Rio Grande do Sul, Brazil*

(Received 18 May 2021; revised 26 July 2022; accepted 11 October 2022; published 28 November 2022)

In conventional Bardeen-Cooper-Schrieffer superconductors, Cooper pairs of electrons of opposite spin (i.e., singlet structure) form the ground state. Equal-spin triplet pairs (ESTPs), as in superfluid ^{3}He, are of great interest for superconducting spintronics and topological superconductivity, yet remain elusive. Recently, odd-parity ESTPs were predicted to arise in (few-)monolayer superconducting $NbSe_2$, from the noncollinearity between the out-of-plane Ising spin-orbit field (due to the lack of inversion symmetry in monolayer $NbSe_2$) and an applied in-plane magnetic field. These ESTPs couple to the singlet order parameter at finite field. Using van der Waals tunnel junctions, we perform spectroscopy of superconducting $NbSe_2$ flakes, of 2–25 monolayer thickness, measuring the quasiparticle density of states (DOS) as a function of applied in-plane magnetic field up to 33 T. In flakes $\lesssim$15 monolayers thick the DOS has a single superconducting gap. In these thin samples, the magnetic field acts primarily on the spin (vs orbital) degree of freedom of the electrons, and superconductivity is further protected by the Ising field. The superconducting energy gap, extracted from our tunneling spectra, decreases as a function of the applied magnetic field. However, in bilayer $NbSe_2$, close to the critical field (up to 30 T, much larger than the Pauli limit), superconductivity appears to be more robust than expected from Ising protection alone. Our data can be explained by the above-mentioned ESTPs.

DOI: 10.1103/PhysRevB.106.184514

I. INTRODUCTION

In both superfluid ^{3}He and conventional Bardeen-Cooper-Schrieffer (BCS) superconductors, the ground state is made up of paired spinful entities, nuclei and electrons, respectively. While the superfluid ^{3}He wave function has a spin triplet structure, conventional superconductors are spin singlet [1].

The question thus arises of the possible existence of triplet superconducting pairs and, in particular, equal-spin triplet pairs (ESTPs, linear combinations of $|\uparrow\uparrow\rangle$ and $|\downarrow\downarrow\rangle$), as have been found in ^{3}He-A [2]. ESTPs are intimately related to topological superconductivity and Majorana edge modes [3]. They are also of great interest for superconducting spintronics, as they can carry spin information without dissipation [4].

ESTPs have recently been predicted to arise in (few-)monolayer superconducting $2H$-$NbSe_2$ (hereinafter $NbSe_2$) in an applied in-plane magnetic field [5], as follows.

Monolayer transition metal dichalcogenides (TMDs), such as $NbSe_2$, with 2H structure lack in-plane crystal inversion symmetry; this gives rise, via the spin-orbit interaction, to an effective out-of-plane magnetic field H_{SO} known as the "Ising (spin-orbit) field" [6–9]. H_{SO} is momentum dependent; in particular, it has opposite sign at the K and K' points of the hexagonal Brillouin zone [10] and a predicted amplitude [11] of $\mu_B H_{SO} = E_{SO} \approx 100$ meV in monolayer $NbSe_2$. As it is time-reversal invariant, H_{SO} does not affect the strength of singlet superconductivity; however, it causes Cooper pair spins to point out of plane [Fig. 1(a)]—unlike conventional superconductors, where Cooper pairs' internal spin axes have no preferred direction.

Thus an applied in-plane magnetic field $H_{||}$ never completely aligns Cooper pair spins in the plane even when the Zeeman energy $E_Z = \mu_B H_{||} \gg E_{SO}$: At zero temperature, the in-plane critical field H_c is expected to diverge logarithmically [6,12]. In agreement with these expectations, TMD superconductors of (few-)monolayer thicknesses obtained by exfoliation [13] or single-layer deposition [14,15] show

*These authors contributed equally to this work.
†Corresponding author: charis.quay@universite-paris-saclay.fr

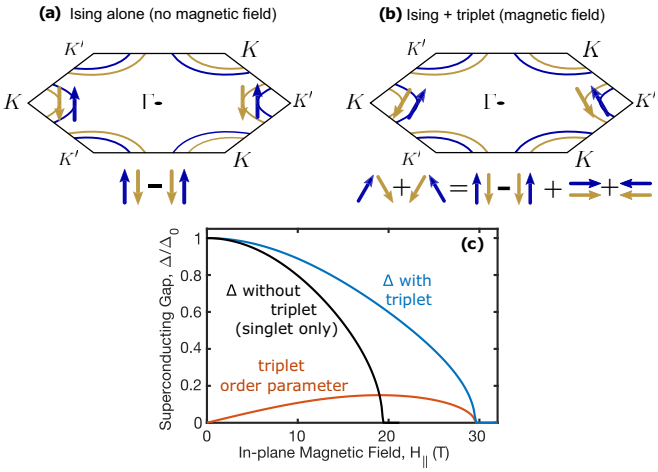

FIG. 1. (a) At zero magnetic field, singlet Cooper pairs are composed of electrons at opposite corners of the hexagonal $NbSe_2$ Brillouin zone (K and K' points). Their spins are pinned out of plane by the Ising field. (b) An in-plane magnetic field partially aligns electron spins orthogonal to the Ising field and gives rise to odd-parity equal-spin triplet pairs [5]. (c) Theoretical superconducting gap as a function of the in-plane magnetic field. Compared with the case where only the Ising field is considered (black curve), superconductivity is even more robust to the in-plane magnetic field, and the Δ vs $H_{||}$ curve has a "flattened" shape at intermediate fields (blue curve). The triplet component of the order parameter (red curve) with spin structure Φ_{tB} survives disorder through its coupling to the singlet component, which has spin structure Φ_s. The temperature used in the calculations is $0.5T_c$, the critical temperature. (See Fig. 4 and the text for details and comparison with data.)

critical fields H_c much larger than $\mu_B H_P = \Delta_0/\sqrt{g}$, the Pauli or paramagnetic limit [16–18]. (Here, μ_B is the Bohr magneton, g is the Landé g factor, and Δ_0 is the superconducting order parameter at zero field.) While inversion symmetry is restored in even-layered $NbSe_2$, the enhancement of H_c persists in bilayer and few-monolayer TMDs, with H_c decreasing monotonically with increasing $NbSe_2$ thickness [16,19,20] and no observation of even-odd effects. This has been attributed to weak interlayer coupling (compared with E_{SO}) [21] and/or spin-layer locking [16].

Both singlet and opposite-spin triplet superconducting order parameters can exist at zero magnetic field, with spin structures $\Phi_s = |\uparrow\downarrow\rangle - |\downarrow\uparrow\rangle$ and $\Phi_t = |\uparrow\downarrow\rangle + |\downarrow\uparrow\rangle$, respectively [22]. For $E_{SO} < E_F$ (the Fermi energy), which is the case here, Φ_t and Φ_s decouple, and Φ_t should not coexist with Φ_s [23,24]. (Φ_t is in any case sensitive to disorder and disappears when the mean free path is shorter than the superconducting coherence length [5].)

The applied in-plane field $H_{||}$, due to its noncollinearity with the Ising field, as well as the momentum dependence of the latter, results in ESTPs with spin structure $\Phi_{tB} = |\downarrow\downarrow\rangle + |\uparrow\uparrow\rangle$ [5,25,26] [Fig. 1(b)]. Φ_{tB} is coupled to Φ_s by the in-plane field, and the critical field is affected by their symbiotic relationship [27]: Φ_{tB} enables Φ_s to survive the magnetic field, while Φ_s enables Φ_{tB} to survive disorder. As a result, in a disordered sample, or even when the temperature $T > T_{ct}$ (the critical temperature associated with Φ_{tB}), the in-plane critical field is higher than it would be for either Φ_s or Φ_{tB} alone, and the dependence of the superconducting gap Δ on the applied field is also affected [Fig. 1(c)].

Very recently, a twofold anisotropy of the critical field, nonlinear transport, and magnetoresistance was observed in few-layer and monolayer $NbSe_2$ devices close to the transition to the normal state [28,29]. These results were also interpreted as coming from unconventional superconductivity: Φ_{tB} triplet components induced by the applied magnetic field and lateral lattice strain can reduce the sixfold rotational symmetry expected from the hexagonal crystal lattice to twofold symmetry [28–30].

Here we report tunneling spectroscopy of few-monolayer $NbSe_2$ devices over a wide range of applied in-plane magnetic fields, up to 30 T. As the magnetic field increases, our measurement of the superconducting gap Δ progressively deviates from the prediction based on pure singlet pairing. We find that this field-induced deviation can be explained by the onset of ESTPs in the form of Φ_{tB} (Fig. 1).

II. RESULTS

We consider a single-band superconductor, with hole pockets at the K and K' points, and include Φ_s and Φ_{tB} correlations. As mentioned above, Φ_{tB} is coupled linearly to Φ_s and is expressed even when $\Delta_{tB} < \Delta s$. If we neglect intervalley scattering, and if a finite pairing interaction is present in the Φ_{tB} channel as suggested by recent density functional theory (DFT) calculations [11], the superconducting energy gap Δ can be obtained from the quasiclassical theory of superconductivity [31]:

$$\Delta = (E_{SO}\Delta_s + E_Z\Delta_{tB})/\sqrt{E_{SO}^2 + E_Z^2}, \tag{1}$$

where Δ_s and Δ_{tB} are the singlet and equal-spin triplet order parameters, respectively.

Here we can see that, compared with the case of Φ_s with Ising protection alone, the coexistence of Δ_{tB} with Δ_s and the coupling between the two can increase the robustness of superconductivity against an applied in-plane magnetic field. In the case where there is no pairing in the equal-spin triplet channel ($\Delta_{tB} = 0$), Δ is reduced by the magnetic field through the factor $E_{SO}/\sqrt{E_{SO}^2 + E_Z^2}$ and vanishes asymptotically, giving the aforementioned logarithmic divergence of the critical field at zero temperature. To obtain the order parameters Δ_s and Δ_{tB} at finite temperature and magnetic field, one has to solve two coupled equations self-consistently [32].

The quasiclassical theory also gives the density of states (DOS), which is found for $E < E_{SO}$ to be simply the BCS DOS, with the gap as in Eq. (1) [31]; unlike two-dimensional (2D) superconductors with low spin-orbit coupling in in-plane fields, the coherence peak is not Zeeman split [33]. In addition, Ising protection gives a sharp coherence peak in the DOS, regardless of the strength of the triplet coupling or the applied magnetic field. Nevertheless, in the presence of intervalley scattering (τ_{iv} being the intervalley scattering time), Ising protection is reduced (due to averaging over valleys with opposite signs of H_{SO}), the DOS is smeared out [24] as in the Abrikosov-Gor'kov theory [34,35], and the divergence of the critical field at zero temperature is regularized [12]. In the

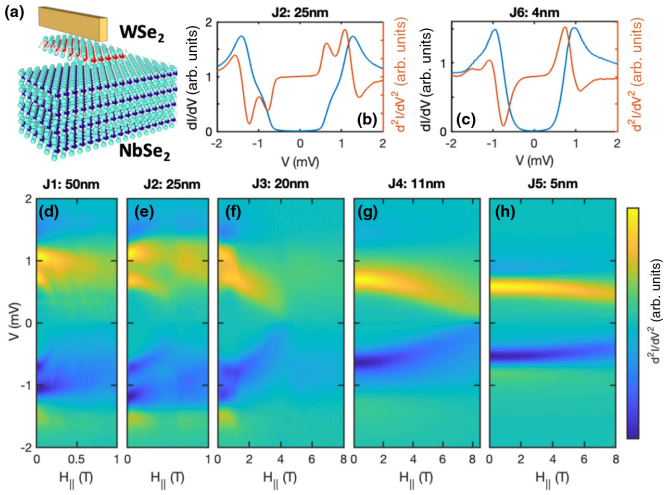

FIG. 2. Tunneling spectroscopy of bulk and few-monolayer $NbSe_2$ through van der Waals barriers. (a) Schematic drawing of the tunnel junction: few-monolayer $NbSe_2$, covered with few-monolayer WSe_2 (or MoS_2) and a Ti/Au electrode. A voltage V is applied between the Ti/Au electrode and the $NbSe_2$, and the current I is measured. (b) Differential conductance ($G = dI/dV$) as a function of V across junction J2 (blue) and d^2I/dV^2 vs V of junction J2 (red). A double peak and a double dip can be seen in d^2I/dV^2, due to the presence of two superconducting gaps. (c) Same as (b), but for junction J6. (d)–(h) Color maps of the magnetic field dependence of the d^2I/dV^2 curves for junctions J1–J5. The double-dip-and-double-peak feature (yellow and blue regions) disappears in thin samples; a single gap is left. Measurements were taken at temperatures of 30–70 mK.

limit of strong intervalley scattering ($E_{SO}^2/\Delta_s \gg 1/\tau_{iv} \gg \Delta_0$) the dependence of Δ on the applied magnetic field becomes similar to that expected from the Abrikosov-Gor'kov theory with the critical field given by $\mu_B H_c = E_{SO}\sqrt{2\Delta\tau_{iv}/\hbar}$ [36]. In our experiment, we do not have strong intervalley scattering as $1/\tau_{iv} \lesssim \Delta_s$ [37].

We fabricate tunnel junctions (junctions J1–J7) on superconducting $NbSe_2$ flakes of 1.2–50 nm thickness. The tunnel barriers are thin flakes of semiconducting WSe_2 or MoS_2 exfoliated by the van der Waals dry transfer technique described in Ref. [38]. A Ti/Au normal counter electrode is then evaporated on the semiconductor leading to the structure shown schematically in Fig. 2(a). An Ohmic contact to the $NbSe_2$ is also fabricated. The typical surface area of the junction is about 1 μm^2, and the resistance in the normal state is >10 kΩ. The critical temperature T_c decreases from $\sim$7.2 K in the thickest flakes to $\sim$2.6 K in the thinnest ones.

Using standard lock-in techniques, we first measure the current I and differential conductance $G = dI/dV$ across the junctions as a function of applied bias voltage V [39] and in-plane magnetic fields $H_{||}$ in dilution refrigerators with base temperatures 30–70 mK. $G(V)$ is proportional to the DOS convolved with the derivative of the Fermi distribution function [40]. Therefore, in principle, the energy resolution of our spectroscopy is given by the temperature and the integrated voltage noise across the junction.

Typical $G(V)$ curves are shown for a 25-nm-thick sample (junction J2) and a six-monolayer sample (junction J6) in Figs. 2(b) and 2(c), respectively. The main differences between these junctions are as follows: (1) the superconducting gap is smaller in the thinner device due to a smaller T_c, and (2) the low-energy shoulder, very clearly seen in the thicker junction, is absent in the thinner one. This is even more apparent in the second derivative of the current as a function of the voltage bias, dG/dV, in Figs. 2(b) and 2(c): The two peaks in junction J2 merge to a single peak in junction J6. This merging was previously observed [38,41], and we now see that it persists in flakes up to 11 nm ($\approx$15 monolayers) thick: The two-gap superconductivity of bulk $NbSe_2$ [42] is lost. This is consistent with band structure calculations for bulk and monolayer $NbSe_2$: Whereas in the bulk three bands cross the Fermi level [43,44] and two superconducting gaps have been observed [38], in the monolayer a single band remains, which crosses the Fermi level twice, resulting in hole pockets at the K and K' points and at the Γ points [11]. A single-band theory thus seems most suitable for the thinnest flakes.

Figures 2(d)–2(h) show the evolution of the dG/dV curves of five junctions (junctions J1–J5) with increasing in-plane magnetic field. Junctions J1 and J2, the thickest, show similar responses to the applied field: The inner peak shifts to lower energies faster than the outer peak. This is consistent with previous experiments and is likely due to the 3D character of the Se-p_z-orbital-derived band at the Γ point, which is associated with the smaller superconducting energy gap, as well as its higher diffusion coefficient [38,45]. For the thinner junctions, junctions J4 and J5, a single gap persists from zero field up to 9 T.

As noted above, the robustness of the gap to applied magnetic fields is expected in thin samples due to Ising protection and drastically reduced orbital depairing (Meissner effect). To significantly reduce the gap and to study the effect of the applied field on the density of states, it is necessary to go to even higher fields.

Therefore we measure two tunnel junctions (junction J6, six monolayers) and (junction J7, bilayer) in in-plane magnetic fields of up to 33 T at 1.3 K (pumped liquid helium). Their critical temperatures are 5.4 K ($H_P = 10.5$ T) and 2.6 K ($H_P = 5$ T), respectively, giving $\Delta/k_B T_c \approx 1.8$, close to the BCS prediction and in agreement with previous studies [38,41]. (See Fig. S2 and inset [31].) Finally, the critical in-plane fields are $H_c = 18$ T for junction J6 and $H_c = 30$ T for junction J7, corresponding to $H_c = 1.5H_P$ and $H_c = 6H_P$, respectively. (See Fig. 4). These junctions had earlier been characterized at 50 mK (dilution refrigerator) at zero magnetic field [Figs. 3(c) and 3(f)]: Hard gaps were observed, pointing to tunneling as the main transport mechanism. These tunnel spectra are well described by a fit to a BCS density of states, broadened by an $\sim$200μeV effective temperature. Though higher than the bath temperature, this broadening does not affect the determination of the energy gap, which can be done with high precision [46].

III. DISCUSSION

The evolution of $G(V)$ with the in-plane magnetic field at 1.3 K is shown in Fig. 3(a) (junction J6) and Fig. 3(d) (junction J7). For clarity, spectra at selected magnetic fields are also shown in Figs. 3(b) and 3(e) together with

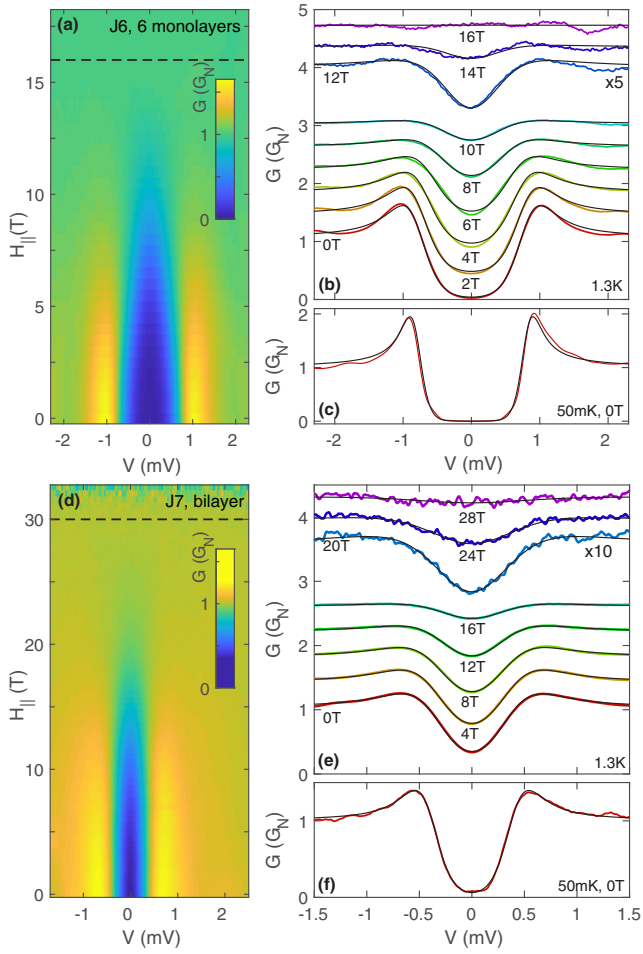

FIG. 3. Differential conductance $G = dI/dV$ as a function of the bias voltage V and of the in-plane magnetic field $H_{||}$ of junction J6 [six monolayers, (a)–(c)] and junction J7 [bilayer, (d)–(f)]. The tunneling spectra are normalized by the normal state conductance, $G_N(V)$, measured above H_c. (a) and (d) Color map of $G(V)$ as a function of field at 1.3 K. The dashed lines indicate the critical fields. (b) and (e) Horizontal slices of the data in the color maps (a) and (d), respectively, showing $G(V)$ at different fields, vertically displaced for clarity. The black curves are fits to an Abrikosov-Gor'kov-like (A-G-like) density of states, with the energy gap and A-G broadening parameter as fitting parameters. (The gap is not determined self-consistently.) (c) and (f) Data at 50 mK and zero magnetic field (red curves) together with the fits obtained using a BCS DOS and an effective temperature (black curves). The superconducting gaps obtained from the fits are 800 and 400 μeV, respectively, while the effective temperatures are 0.9 and 1 K, respectively.

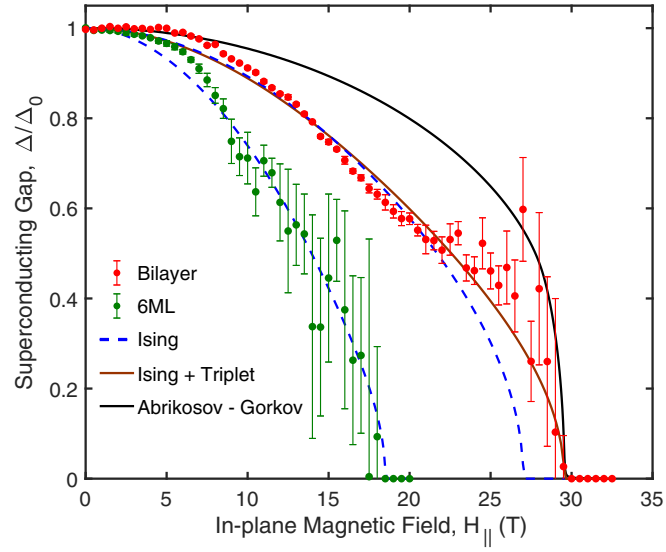

FIG. 4. Normalized superconducting gap as a function of the in-plane magnetic field $\Delta(H_{||})$ obtained from the fits of the quasiparticle density of states in Fig. 3. The error bars were obtained following the procedure described in Supplemental Material Sec. I A. The blue dashed curves are a fit of experimental data using the Ising theory alone. Here, $E_{SO} = 14.45T_{cs}$ (with $T_{cs} = 2.6$ K) for the bilayer sample and $E_{SO} = 2.21T_{cs}$ (with $T_{cs} = 5.4$ K) for the six-monolayer (6ML) sample. In brown is the Ising theory with an equal-spin triplet component of the order parameter as described in the text. Here, $E_{SO} = 9.62T_{cs}$ and $T_{ct} = 0.05T_{cs}$, with $T_{cs} = 2.6$ K. Finally, the solid black curve is calculated using the Ising theory with strong disorder (equivalent to the Abrikosov-Gor'kov theory). In all cases, the critical field is constrained to be the experimental one.

an Abrikosov-Gor'kov-like density of states with a field-dependent broadening parameter [34,47], convolved with a Fermi function to account for the temperature. The fits account very well for the experimental data.

The superconducting gaps obtained from these fits are shown as a function of the in-plane magnetic field in Fig. 4 and compared with theory.

For the six-monolayer device, a simple Ising model accounts for the data reasonably well (Fig. 4, leftmost dashed blue curve). The fitting parameters are given in the caption of the figure.

Focusing on the thinner, bilayer device (junction J7), we see that the Ising theory alone without triplet pairing fits the data reasonably well up to about 20 T, but not close to the critical field, where the superconducting energy gap is more robust than expected (Fig. 4, rightmost dashed blue curve).

This key experimental finding is suggestive of a second order parameter, which is revealed as the dominant order parameter disappears [23]. Indeed, introducing a small ESTP component of the gap (triplet model), a better fit of the overall experimental data is obtained (Fig. 4, brown curve). The temperature of the experiment (1.3 K) is above the triplet critical temperature ($T_{ct} = 0.05T_{cs} = 130$ mK, obtained from the fit). Therefore the ESTP order parameter Δ_{tB} exists only through its coupling with the singlet order parameter Δ_s, and its main effect is to enhance the critical field through the coupling with the singlet order parameter. In addition, the triplet subdominant component also renders the gap vs field dependence more linear [Fig. 1(c)].

Our fit also gives $E_{SO} = 9.62T_{cs}$ ($\sim$2.2 meV). This is a lower bound for E_{SO}, as intervalley ($K - K'$) scattering is not taken into account. If it is, higher values of E_{SO} will have to be used to arrive at the same $H_{||}^c$, but the shape of the $\Delta(H_{||})$ curve is similar. Furthermore, we note that the shape of $\Delta(H_{||})$ in the triplet model is by construction impervious to intravalley scattering. Our E_{SO} value is consistent with the upper bound for E_{SO} given by angle-resolved photoemission spectroscopy (ARPES) measurements, which indicate $E_{SO} \lesssim 20$ meV (the

measurement resolution), significantly lower than theoretical predictions [48].

For completeness, we also show the Ising theory with strong intervalley scattering (equivalent to Abrikosov-Gor'kov theory), where the only fitting parameter is the critical field (Fig. 4, black curve). This does not fit the data at all: The experimental Δ is consistently smaller than that predicted by the theory, which also fails to reproduce the "linear" part of the curve at intermediate fields.

At present, much of the literature on quantum transport in few-layer $NbSe_2$ includes only the hole pockets at the K and K' points, as we did, even though there is also a hole pocket at the Γ point [11]. In Supplemental Material Secs. II C and II D, we consider models which include only Φ_s, and $K-\Gamma$ and K'-Γ coupling and neglect all triplet order parameters. These are found not to fit our data well, given the known level of disorder in the sample, thus strengthening the case for the ESTP interpretation [49].

Regarding ESTPs, we note that, within the scenarios of Refs. [28,29] mentioned earlier, the triplet order parameters allowed by symmetry such as Φ_{tB} have to be nearly degenerate with the leading singlet order parameter. Attraction in the triplet channel is supported by recent density functional theory (DFT) calculations [11]; however, there is at present no evidence of near degeneracy between triplet and singlet channels. Our interpretation does not require near degeneracy, and the singlet-triplet coupling comes from a clear microscopic mechanism (the in-plane magnetic field), which is quantitatively accounted for both in the theory and in the analysis of the experimental data.

While previous reports on Andreev spectroscopy experiments have shown a reduction of the gap consistent with field-induced depairing in the presence of Ising protection [50], our hard-gap tunnel junctions allow a nuanced and quantitative analysis of the possible microscopic mechanisms for the enhancement of the critical field, pointing to the presence of equal-spin triplet superconductivity.

Further study at even lower temperatures, independent measurements of E_{SO}, independent estimates of the K-Γ and K'-Γ coupling from theory or experiment, and momentum-selective barriers would be helpful to unambiguously confirm the existence of ESTPs in $NbSe_2$.

IV. MATERIALS AND METHODS

Especially at high magnetic fields, special care was taken to ensure that the applied magnetic field is parallel to the flakes. It is aligned to better than $\sim 1^\circ$. In addition, we checked that the voltage noise due to mechanical vibrations is lower than that from the thermal broadening [51].

The data sets generated and/or analyzed during the current study are available from the corresponding author upon reasonable request.

ACKNOWLEDGMENTS

We acknowledge valuable discussions with Pascal Simon and Freek Massee and thank the latter for a careful reading of the manuscript. This work was funded by a Maimonides-Israel grant from the Israeli-French High Council for Scientific and Technological Research; JCJC (SPINOES), PIRE (HYBRID), and PRC (TRIPRES) grants from the French Agence Nationale de Recherche; European Research Council Starting Grant No. ERC-2014-STG 637928 (TUNNEL); Israel Science Foundation Grants No. 861/19 and No. 2665/20, and the Laboratoire d'Excellence LANEF in Grenoble (ANR10-LABX-51-01). T.D. is grateful to the Azrieli Foundation for an Azrieli Fellowship. Part of this work has been performed at the Laboratoire National de Champs Magnétiques Intenses (LNCMI), a member of the European Magnetic Field Laboratory (EMFL).

[1] J. F. Annett, *Superconductivity, Superfluids, and Condensates*, 1st ed. (Oxford University Press, Oxford, 2004).

[2] A. J. Leggett, Nobel Lecture: Superfluid ^{3}He: the early days as seen by a theorist, Rev. Mod. Phys. **76**, 999 (2004).

[3] S. M. Frolov, M. J. Manfra, and J. D. Sau, Topological superconductivity in hybrid devices, Nat. Phys. **16**, 718 (2020).

[4] K. Ohnishi, S. Komori, G. Yang, K.-R. Jeon, L. A. B. Olde Olthof, X. Montiel, M. G. Blamire, and J. W. A. Robinson, Spin-transport in superconductors, Appl. Phys. Lett. **116**, 130501 (2020).

[5] D. Möckli and M. Khodas, Ising superconductors: Interplay of magnetic field, triplet channels, and disorder, Phys. Rev. B **101**, 014510 (2020).

[6] P. A. Frigeri, D. F. Agterberg, and M. Sigrist, Spin susceptibility in superconductors without inversion symmetry, New J. Phys. **6**, 115 (2004).

[7] L. P. Gor'kov and E. I. Rashba, Superconducting 2D System with Lifted Spin Degeneracy: Mixed Singlet-Triplet State, Phys. Rev. Lett. **87**, 037004 (2001).

[8] Y. Saito, Y. Nakamura, M. S. Bahramy, Y. Kohama, J. Ye, Y. Kasahara, Y. Nakagawa, M. Onga, M. Tokunaga, T. Nojima, Y. Yanase, and Y. Iwasa, Superconductivity protected by spin–valley locking in ion-gated MoS_2, Nat. Phys. **12**, 144 (2016).

[9] J. M. Lu, O. Zheliuk, I. Leermakers, N. F. Q. Yuan, U. Zeitler, K. T. Law, and J. T. Ye, Evidence for two-dimensional Ising superconductivity in gated MoS_2, Science **350**, 1353 (2015).

[10] X. Xu, W. Yao, D. Xiao, and T. F. Heinz, Spin and pseudospins in layered transition metal dichalcogenides, Nat. Phys. **10**, 343 (2014).

[11] D. Wickramaratne, S. Khmelevskyi, D. F. Agterberg, and I. I. Mazin, Ising Superconductivity and Magnetism in $NbSe_2$, Phys. Rev. X **10**, 041003 (2020).

[12] S. Ilić, J. S. Meyer, and M. Houzet, Enhancement of the Upper Critical Field in Disordered Transition Metal Dichalcogenide Monolayers, Phys. Rev. Lett. **119**, 117001 (2017).

[13] Q. H. Wang, K. Kalantar-Zadeh, A. Kis, J. N. Coleman, and M. S. Strano, Electronics and optoelectronics of

two-dimensional transition metal dichalcogenides, Nat. Nanotechnol. **7**, 699 (2012).

[14] T. Zhang, P. Cheng, W.-J. Li, Y.-J. Sun, G. Wang, X.-G. Zhu, K. He, L. Wang, X. Ma, X. Chen, Y. Wang, Y. Liu, H.-Q. Lin, J.-F. Jia, and Q.-K. Xue, Superconductivity in one-atomic-layer metal films grown on Si(111), Nat. Phys. **6**, 104 (2010).

[15] Q. Fan, W. H. Zhang, X. Liu, Y. J. Yan, M. Q. Ren, R. Peng, H. C. Xu, B. P. Xie, J. P. Hu, T. Zhang, and D. L. Feng, Plain *s*-wave superconductivity in single-layer FeSe on $SrTiO_3$ probed by scanning tunnelling microscopy, Nat. Phys. **11**, 946 (2015).

[16] X. Xi, Z. Wang, W. Zhao, J.-H. Park, K. T. Law, H. Berger, L. Forró, J. Shan, and K. F. Mak, Ising pairing in superconducting $NbSe_2$ atomic layers, Nat. Phys. **12**, 139 (2016).

[17] Y. Liu, Z. Wang, X. Zhang, C. Liu, Y. Liu, Z. Zhou, J. Wang, Q. Wang, Y. Liu, C. Xi, M. Tian, H. Liu, J. Feng, X. C. Xie, and J. Wang, Interface-Induced Zeeman-Protected Superconductivity in Ultrathin Crystalline Lead Films, Phys. Rev. X **8**, 021002 (2018).

[18] At the Pauli limit, the paramagnetic state of spin-aligned quasiparticles becomes more energetically favorable than the superconducting ground state [52,53]. In the absence of spin-orbit coupling, H_P is thus the expected H_c for thin superconductors, where the Meissner effect can be neglected.

[19] S. C. de la Barrera, M. R. Sinko, D. P. Gopalan, N. Sivadas, K. L. Seyler, K. Watanabe, T. Taniguchi, A. W. Tsen, X. Xu, D. Xiao, and B. M. Hunt, Tuning Ising superconductivity with layer and spin–orbit coupling in two-dimensional transition-metal dichalcogenides, Nat. Commun. **9**, 1427 (2018).

[20] D. E. Prober, R. E. Schwall, and M. R. Beasley, Upper critical fields and reduced dimensionality of the superconducting layered compounds, Phys. Rev. B **21**, 2717 (1980).

[21] A. M. Jones, H. Yu, J. S. Ross, P. Klement, N. J. Ghimire, J. Yan, D. G. Mandrus, W. Yao, and X. Xu, Spin–layer locking effects in optical orientation of exciton spin in bilayer WSe_2, Nat. Phys. **10**, 130 (2014).

[22] M. Smidman, M. B. Salamon, H. Q. Yuan, and D. F. Agterberg, Superconductivity and spin–orbit coupling in non-centrosymmetric materials: A review, Rep. Prog. Phys. **80**, 036501 (2017).

[23] D. Rainer, H. Burkhardt, M. Fogelström, and J. A. Sauls, Andreev bound states, surfaces and subdominant pairing in high T_c superconductors, J. Phys. Chem. Solids **59**, 2040 (1998).

[24] M. Haim, D. Möckli, and M. Khodas, Signatures of triplet correlations in density of states of Ising superconductors, Phys. Rev. B **102**, 214513 (2020).

[25] G. Tang, C. Bruder, and W. Belzig, Magnetic Field-Induced "Mirage" Gap in an Ising Superconductor, Phys. Rev. Lett. **126**, 237001 (2021).

[26] Y. Nakamura and Y. Yanase, Odd-parity superconductivity in bilayer transition metal dichalcogenides, Phys. Rev. B **96**, 054501 (2017).

[27] D. Möckli and M. Khodas, Magnetic-field induced $s + if$ pairing in Ising superconductors, Phys. Rev. B **99**, 180505(R) (2019).

[28] A. Hamill, B. Heischmidt, E. Sohn, D. Shaffer, K.-T. Tsai, X. Zhang, X. Xi, A. Suslov, H. Berger, L. Forró, F. J. Burnell, J. Shan, K. F. Mak, R. M. Fernandes, K. Wang, and V. S. Pribiag, Unexpected two-fold symmetric superconductivity in few-layer $NbSe_2$, Nat. Phys. **17**, 949 (2021).

[29] C.-w. Cho, J. Lyu, L. An, T. Han, K. T. Lo, C. Y. Ng, J. Hu, Y. Gao, G. Li, M. Huang, N. Wang, J. Schmalian, and R. Lortz, Nodal and Nematic Superconducting Phases in $NbSe_2$ Monolayers from Competing Superconducting Channels, Phys. Rev. Lett. **129**, 087002 (2022).

[30] M. Haim, A. Levchenko, and M. Khodas, Mechanisms of in-plane magnetic anisotropy in superconducting $NbSe_2$, Phys. Rev. B **105**, 024515 (2022).

[31] See Supplemental Material at http://link.aps.org/supplemental/10.1103/PhysRevB.106.184514 for details.

[32] See Supplemental Material Sec. II for details of this calculation.

[33] R. Meservey, P. M. Tedrow, and P. Fulde, Magnetic Field Splitting of the Quasiparticle States in Superconducting Aluminum Films, Phys. Rev. Lett. **25**, 1270 (1970).

[34] A. A. Abrikosov and L. P. Gor'kov, Contribution to the theory of superconducting alloys with paramagnetic impurities, Sov. Phys. JETP **12**, 1243 (1961).

[35] R. C. Bruno and B. B. Schwartz, Magnetic field splitting of the density of states of thin superconductors, Phys. Rev. B **8**, 3161 (1973).

[36] See Supplemental Material Sec. II and references therein [5,11,13,24,25,27,34,54–61] for theoretical details.

[37] See Supplemental Material Sec. I C and references therein [12,19] for details on this estimate.

[38] T. Dvir, F. Massee, L. Attias, M. Khodas, M. Aprili, C. H. L. Quay, and H. Steinberg, Spectroscopy of bulk and few-layer superconducting $NbSe_2$ with van der Waals tunnel junctions, Nat. Commun. **9**, 598 (2018).

[39] I. Giaever, Energy Gap in Superconductors Measured by Electron Tunneling, Phys. Rev. Lett. **5**, 147 (1960).

[40] M. Tinkham, *Introduction to Superconductivity*, 2nd ed. (Dover, Mineola, 1996).

[41] E. Khestanova, J. Birkbeck, M. Zhu, Y. Cao, G. L. Yu, D. Ghazaryan, J. Yin, H. Berger, L. Forró, T. Taniguchi, K. Watanabe, R. V. Gorbachev, A. Mishchenko, A. K. Geim, and I. V. Grigorieva, Unusual suppression of the superconducting energy gap and critical temperature in atomically thin $NbSe_2$, Nano Lett. **18**, 2623 (2018).

[42] Y. Noat, J. A. Silva-Guillén, T. Cren, V. Cherkez, C. Brun, S. Pons, F. Debontridder, D. Roditchev, W. Sacks, L. Cario, P. Ordejón, A. García, and E. Canadell, Quasiparticle spectra of $NbSe_2$: Two-band superconductivity and the role of tunneling selectivity, Phys. Rev. B **92**, 134510 (2015).

[43] M. D. Johannes, I. I. Mazin, and C. A. Howells, Fermi-surface nesting and the origin of the charge-density wave in $NbSe_2$, Phys. Rev. B **73**, 205102 (2006).

[44] T. Yokoya, T. Kiss, A. Chainani, S. Shin, M. Nohara, and H. Takagi, Fermi surface sheet-dependent superconductivity in $2H$-$NbSe_2$, Science **294**, 2518 (2001).

[45] T. Dvir, M. Aprili, C. H. L. Quay, and H. Steinberg, Tunneling into the vortex state of $NbSe_2$ with van der Waals junctions, Nano Lett. **18**, 7845 (2018).

[46] See Supplemental Material Secs. I A and I B and references therein [34,41,62–69] for details of our analysis of the tunneling spectra.

[47] R. V. A. Srivastava and W. Teizer, Analytical density of states in the Abrikosov-Gorkov theory, Solid State Commun. **145**, 512 (2008).

[48] C.-Z. Xu, X. Wang, P. Chen, D. Flötotto, J. A. Hlevyack, M.-K. Lin, G. Bian, S.-K. Mo, and T.-C. Chiang, Experimental and

theoretical electronic structure and symmetry effects in ultrathin $NbSe_2$ films, Phys. Rev. Mater. **2**, 064002 (2018).

[49] A more complete theory (beyond our present computational capabilities) would include both K and K' pockets and Γ pockets [which exist but do not give the desired $\Delta(H_{||})$] as well as Φ_{tB} [which should give the observed "shoulder" in $\Delta(H_{||})$]. In all cases, triplets would be required.

[50] E. Sohn, X. Xi, W.-Y. He, S. Jiang, Z. Wang, K. Kang, J.-H. Park, H. Berger, L. Forró, K. T. Law, J. Shan, and K. F. Mak, An unusual continuous paramagnetic-limited superconducting phase transition in 2D $NbSe_2$, Nat. Mater. **17**, 504 (2018).

[51] See Supplemental Material Sec. I A and references therein [30,38,41,70] for details of sample fabrication and magnetic field compensation.

[52] A. M. Clogston, Upper Limit for the Critical Field in Hard Superconductors, Phys. Rev. Lett. **9**, 266 (1962).

[53] P. Fulde, High field superconductivity in thin films, Adv. Phys. **22**, 667 (1973).

[54] K. Maki and T. Tsuneto, Pauli paramagnetism and superconducting state, Prog. Theor. Phys. **31**, 945 (1964).

[55] H. Suhl, B. T. Matthias, and L. R. Walker, Bardeen-Cooper-Schrieffer Theory of Superconductivity in the Case of Overlapping Bands, Phys. Rev. Lett. **3**, 552 (1959).

[56] Z. Y. Zhu, Y. C. Cheng, and U. Schwingenschlögl, Giant spin-orbit-induced spin splitting in two-dimensional transition-metal dichalcogenide semiconductors, Phys. Rev. B **84**, 153402 (2011).

[57] V. G. Kogan and J. Schmalian, Ginzburg-Landau theory of two-band superconductors: Absence of type-1.5 superconductivity, Phys. Rev. B **83**, 054515 (2011).

[58] D. Wickramaratne, M. Haim, M. Khodas, and I. I. Mazin, Magnetism-driven unconventional effects in Ising superconductors: Role of proximity, tunneling, and nematicity, Phys. Rev. B **104**, L060501 (2021).

[59] W. L. McMillan, Tunneling Model of the Superconducting Proximity Effect, Phys. Rev. **175**, 537 (1968).

[60] D. Sticlet and C. Morari, Topological superconductivity from magnetic impurities on monolayer $NbSe_2$, Phys. Rev. B **100**, 075420 (2019).

[61] A. Kaiser and M. Zuckermann, McMillan model of the superconducting proximity effect for dilute magnetic alloys, Phys. Rev. B **1**, 229 (1970).

[62] S. Skalski, O. Betbeder-Matibet, and P. Weiss, Properties of Superconducting Alloys Containing Paramagnetic Impurities, Phys. Rev. **136**, A1500 (1964).

[63] R. C. Dynes, V. Narayanamurti, and J. P. Garno, Direct Measurement of Quasiparticle-Lifetime Broadening in a Strong-Coupled Superconductor, Phys. Rev. Lett. **41**, 1509 (1978).

[64] F. Herman and R. Hlubina, Microscopic interpretation of the Dynes formula for the tunneling density of states, Phys. Rev. B **94**, 144508 (2016).

[65] S. Hörhold, J. Graf, M. Marganska, and M. Grifoni, Two bands Ising superconductivity from Coulomb interactions in monolayer $NbSe_2$, arXiv:2206.06645.

[66] M. H. Fischer, M. Sigrist, and D. F. Agterberg, Superconductivity without Inversion and Time-Reversal Symmetries, Phys. Rev. Lett. **121**, 157003 (2018).

[67] P. Hlobil, J. Jandke, W. Wulfhekel, and J. Schmalian, Tracing the Electronic Pairing Glue in Unconventional Superconductors via Inelastic Scanning Tunneling Spectroscopy, Phys. Rev. Lett. **118**, 167001 (2017).

[68] M. A. Reed, Inelastic electron tunneling spectroscopy, Mater. Today **11**, 46 (2008).

[69] P. B. Littlewood and C. M. Varma, Amplitude collective modes in superconductors and their coupling to charge-density waves, Phys. Rev. B **26**, 4883 (1982).

[70] A. W. Tsen, B. Hunt, Y. D. Kim, Z. J. Yuan, S. Jia, R. J. Cava, J. Hone, P. Kim, C. R. Dean, and A. N. Pasupathy, Nature of the quantum metal in a two-dimensional crystalline superconductor, Nat. Phys. **12**, 208 (2016).